SEISMIC RETROFIT OF SHEAR-CRITICAL R.C. BEAMS USING CFRP

M. A. Colalillo [1] S.A. Sheikh [2]

[1] Department of Civil Engineering, University of Toronto, Canada
[2] Department of Civil Engineering, University of Toronto, Canada

Keywords: shear strengthening, seismic retrofit, reverse shear, cyclic loading, carbon FRP

1 INTRODUCTION

Research on the seismic performance of FRP-retrofitted reinforced concrete (RC) members has primarily focused on strengthening of columns and beam-column joints to promote a ductile collapse mechanism. However, it is also imperative that beams have sufficient shear capacity to develop plastic hinges in flexure under seismic loading. Many existing RC structures in seismic regions are inadequately designed for shear and at risk of catastrophic brittle failure during an earthquake. One such example is the cement pre-heater tower described in [1] that was designed using outdated shear provisions. The tower had shear-critical beams and was at risk of collapse during an earthquake. Testing performed on a scaled-down frame of the tower showed that shear retrofit of the beams with FRP was effective at changing the system failure mode to flexure. Unfortunately, limited information was gathered concerning FRP failure since the beams no longer failed in shear. Thus, further testing was warranted to evaluate the complete response of FRP-retrofitted shear-critical beams under simulated earthquake loading.

The objective of this research is to quantify the shear strength improvement provided by various FRP wrap configurations when applied to large-size beams with different amounts of internal transverse steel. Since FRP shear capacity formulations by CSA [2] and ACI [3] were derived from the results of static testing, their validity under seismic loading is of importance. Experimental results are used to verify the accuracy of code predicted FRP shear capacities and design code strain limits.

2 EXPERIMENTAL PROGRAM

2.1 Specimen Details

An experimental program was undertaken in which fifteen reinforced concrete beams were tested in a three-point bending configuration under reversed cyclic loading. The beams were divided into three series based on the amount of internal transverse steel used: no transverse steel (S0 series), less than the minimum amount (S5 series) as required by [2], and twice that amount (S2 series). Transverse steel consisted of closed stirrups made from U.S. #3 bars (area = 71mm^2), having a yield stress of 501 MPa at a strain of 0.25%. A stirrup spacing of 500 mm was provided for the S5 series and 250 mm for the S2 series.

All beams were 650 mm deep, 400 mm wide and 3.6 m long. They were doubly reinforced in flexure with eight 30M longitudinal bars (area = 700 mm^2) at top and bottom. The steel yield stress was 481 MPa at a strain of 0.25%. The shear span-to-depth ratio (a/d) was 3.1. The beams were cast in three separate batches and tested about three months after each casting. The concrete compressive strength at the time of beam testing varied between 48 MPa and 53 MPa.

For each series, one beam was tested unretrofitted as the control. FRP was applied to the remaining specimens in each series as follows (Fig. 1): U-wrap with strips (US), U-wrap with continuous sheets along the beam length (UA), closed or completely wrapped with strips (CS), and completely wrapped with continuous sheets (CA). The U-wraps were applied along the sides and bottom face of the beams, while the complete wraps covered all four faces of the beams with 100 mm overlap on the top face. Strips were 100 mm wide and spaced at 200 mm centre-to-centre. A 100 mm wide longitudinal band was applied along the top of U-wrap strips to increase the bonding area and prevent premature debonding. To prevent premature failure caused by stress concentrations in the FRP, the beams were cast with rounded edges of 38 mm diameter [2]. The FRP system used was composed of Tyfo® SCH-41 unidirectional carbon-fibre fabric and Tyfo® S Epoxy. The FRP was applied transversely to the beam longitudinal axis as a single layer with 1.0 mm thickness. The tensile strength and rupture strain of FRP were 1006 MPa and 1.07%, respectively.

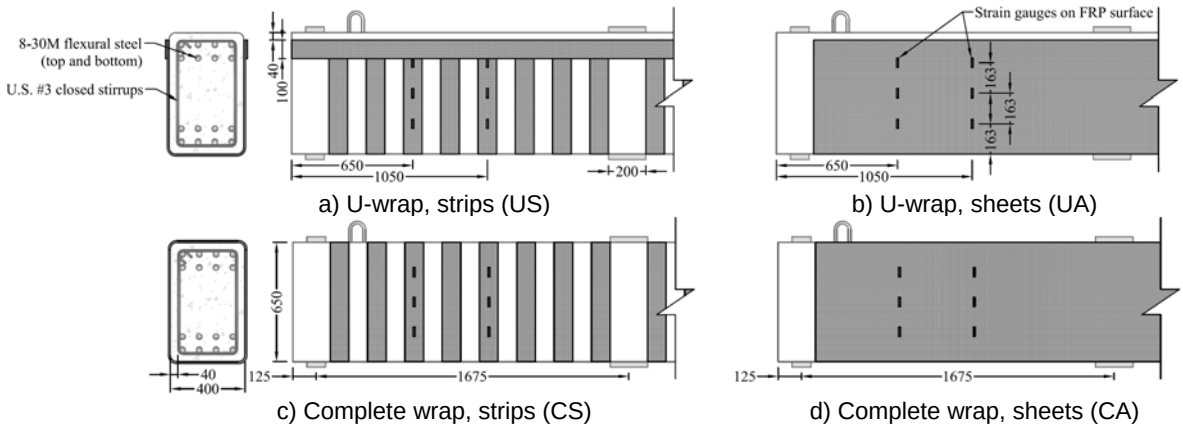

a) U-wrap, strips (US) b) U-wrap, sheets (UA)

c) Complete wrap, strips (CS) d) Complete wrap, sheets (CA)

Fig. 1 Specimen FRP details.

2.2 Testing Details

All specimens were tested under displacement control. Load values were used to define the end of cycles prior to flexural yielding in beams. The control specimens were cycled twice at ±0.5 and ±0.75 times the approximate predicted monotonic shear failure load. For retrofitted specimens, the loading scheme consisted of two cycles at each increasing interval of ±0.25 times the failure load of the control specimen for a particular series. For those retrofitted beams that failed in flexure, the load excursions beyond yield were defined in increments of the yield displacement.

Steel assemblies were used to hold the specimens down to the strong floor, with roller bearings and plaster-filled bags placed in-between to provide a simple-support condition. A similar assembly was used at mid-span to connect the specimens to the MTS actuator head. Steel clamps were placed over one span to improve shear strength and ensure failure in the more heavily instrumented span. Linear variable displacement transducers (LVDT) were used to measure the relative mid-span displacement with respect the supports.

3 RESULTS

3.1 Overall Response

Due to space limits, only the results of the S5 series are presented herein. For these specimens the ultimate shear capacity and mid-span displacement at FRP failure are provided in Table 1. The S5 control specimen failed in shear at 415 kN, about 25% larger than predicted using sectional shear models [2], which may be due to effects such as dowel action and tension stiffening that are neglected in the analysis. The addition of FRP clearly improves shear strength beyond that of the control, providing strength increases of 25% for U-wrap with strips to 114% for completely wrapped with sheets. Although not shown, strength increases for the S5 series were higher than increases of the S2 series, while lower than increases of the S0 series. Thus, the shear strength improvement offered by the FRP is lower when more internal transverse steel is present.

Table 1 S5 series strengthening details and test results.

Specimen	FRP strengthening	Shear strength (kN)	Shear strength increase (%)	Mid-span displacement at FRP failure (mm)	Failure mode
S5	Control	415	-	7.7	Shear
S5-US	U-wrap, strips	518	25	7.6	Shear, FRP debonding
S5-UA	U-wrap, sheets	622	50	9.1	Shear, FRP debonding
S5-CS	Complete wrap, strips	725	75	12.6	Shear, FRP rupture
S5-CA	Complete wrap, sheets	888	114	69.0	Flexure, FRP rupture

Response curves depicting shear force versus mid-span displacement are provided in Fig. 2. For all specimens, first flexural cracking occurred at a shear of about 100 kN, causing an initial change in stiffness. The onset of shear cracking is also apparent due to a change in stiffness, but its occurrence is dependent on the wrap scheme applied. FRP stiffened the beams such that further change in stiffness was minimal after first shear cracking and before longitudinal steel yielding.

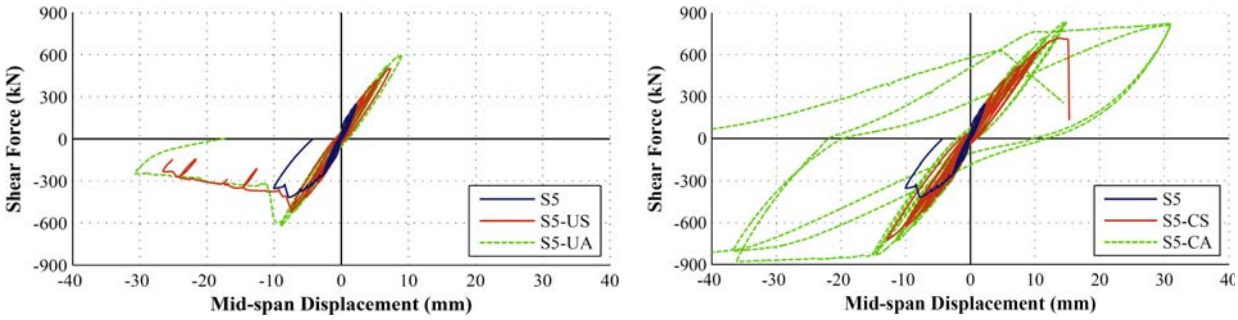

a) U-wrap specimens b) Completely wrapped specimens

Fig. 2 Shear-displacement response curves for S5 series specimens.

The U-wrap specimens failed by debonding due to failure within the concrete matrix, as pieces of concrete were attached to the delaminated FRP. After failure of the U-wrap specimens, the response curves drop to a load plateau (Fig. 2a), indicating some residual capacity associated with the longitudinal steel. This is not apparent among the completely wrapped specimens, which were subjected to more severe concrete damage at higher load levels (Fig. 2b). Completely wrapped specimens failed due to FRP rupture, which was sudden in the case of S5-CS. The specimen with completely wrapped sheets (S5-CA) experienced flexural yielding at a shear of 850 kN and mid-span displacement of 15 mm. After further cycling, catastrophic brittle failure of S5-CA occurred when FRP ruptured at a beam mid-span displacement about 4 times the yield displacement.

3.2 Strain Gauge Readings

The FRP surface was strain gauged at three locations along the beam corresponding to 650 mm, 850 mm, and 1050 mm away from the end (Fig. 1). At each of these locations, gauges were placed at three heights to obtain an average strain at each section. Significant straining of the transverse steel and FRP began after first shear cracking. Transverse steel strains were sufficiently high for stirrup yielding to occur prior to specimen failure. The maximum strain measured in the U-wrap FRP before the specimens failed ranged from 0.3% to 0.4%, with no clear difference observed between strips and sheets. This agrees well with predicted failure strains from CSA [2] and ACI [3], which are slightly higher than strains predicted by others [4-6]. Completely wrapped FRP was found to fail at strains greater than 0.6%. This is close to the predicted failure strains from [4-6], which vary between 0.64% and 0.7%, while CSA [2] and ACI [3] impose a strain limit of 0.4% for completely wrapped beams.

3.3 FRP Shear Capacity

To eliminate the inconsistencies associated with the prediction of RC shear strength, the shear capacity of FRP is evaluated separately. Table 2 provides the predicted FRP shear strengths calculated using several formulations [2-6], in which the effective FRP strain values vary. The FRP effective depth was taken as 451 mm and 491 mm for U-wrap and completely wrapped specimens, respectively. References [2,4-6] incorporate a variable crack angle, although [4-6] suggest using 45° for design, unless a more precise calculation is made. ACI [3] neglects the variation in crack angle, assuming 45°. Specimens S5, S5-US, and S5-CS were observed to have crack angles of 45°, 43°, and 40°, respectively, while angles of about 37° were observed for S5-UA and S5-CA (Fig. 3). Since several primary cracks formed, it is difficult to determine the precise angle. Thus, a range of angles is shown in Table 2 to emphasise the influence on predicted FRP strengths.

a) S5-US b) S5-UA c) S5-CA

Fig. 3 Specimens after failure with FRP removed.

The shear capacity of the FRP was experimentally derived by two methods to attain an upper and lower bound as a basis for comparison to predicted strengths. Taking the difference in shear capacity between a retrofitted specimen and the control ($V_{retrofit}$ - $V_{control}$) provides an indication of the increase in shear capacity due to the presence of the FRP. However, this increase is not attributed to the FRP alone, since the concrete and transverse steel shear contributions may also change. The FRP shear capacity derived from strain readings ($V_{strains}$) was also calculated using [2], wherein the maximum of FRP average strains measured from three locations was used.

Table 2 FRP shear strengths with varied crack angle.

	Specimen:	S5-US				S5-UA				S5-CS			
	Crack angle:	45	**43**	40	37	45	43	40	**37**	45	43	**40**	37
Predicted	ACI 440.2R-08 [3]	147				295				185			
	CSA-S6-06 [2]	147	158	176	195	295	316	352	392	185	199	221	246
	Chen & Teng [4,5]	104	111	124	138	147	157	175	195	297	319	354	394
	CNR-DT 200/2004 [6]	103	111	123	137	198	212	236	263	323	347	385	429
Exp	$V_{retrofit}$ - $V_{control}$		103						207			310	
	$V_{strains}$		129						250			328	

The effect of varying the crack angle is apparent among predictions [4-6], which in most cases are close to experimentally derived FRP shear strengths when observed crack angles were used. The ACI [3] predictions are the least accurate as they neglect the variable crack angle. Although the CSA [2] formulations incorporate a variable crack angle, the predictions for U-wrap specimens are overestimated, while the FRP strength of the completely wrapped specimen (S5-CS) is greatly underestimated due to the imposed strain limit of 0.4%.

4 CONCLUSIONS

CFRP retrofit enhanced the shear strength of beams under simulated earthquake loads by up to 114% of the control specimen strength. FRP stiffened the beams and allowed for relatively elastic behavior prior to shear failure. This produced shear strengths that were comparable to monotonic predictions, showing that the FRP performance is not affected by cyclic loading. The completely wrapped specimens with sheets had sufficient shear strength to allow for flexural yielding, followed by FRP rupture at beam deflections over 4 times larger than the beam yield displacement. CSA [2] and ACI [3] strain limits for debonding failure were adequate, while limiting the FRP strain at failure to 0.4% for completely wrapped beams was overly conservative. Shear formulations [4-6] produced reasonable FRP shear strength predictions if the observed crack angles were used in the analysis.

ACKNOWLEDGEMENTS

Funding for this research was provided by ISIS Canada Network and the Natural Sciences and Engineering Research Council of Canada. Assistance from the technical staff of the University of Toronto Structural Laboratories is gratefully acknowledged.

REFERENCES

[1] Duong, K.V., Sheikh, S.A. and Vecchio, F.J., “Seismic Behaviour of Shear-Critical Reinforced Concrete Frame: Experimental Investigation”, *ACI Structural Journal*, 104, 3, 2007, pp 304-313.

[2] CSA. “CAN/CSA-S6-06 - Canadian Highway Bridge Design Code”, Canadian Standards Association, 2006, 800 pp.

[3] ACI. “ACI440.2R-08 - Guide for Design and Construction of Externally Bonded FRP Systems for Strengthening Concrete Structures”, American Concrete Institute, Committee 440, 2008.

[4] Chen, J.F. and Teng, J.G. “Shear Capacity of FRP-Strengthened RC Beams: FRP Debonding”, *Construction and Building Materials*, 17, 2003, pp 27-41.

[5] Chen, J.F. and Teng, J.G. “Shear Capacity of FRP-Strengthened RC Beams: FRP Rupture”, *ASCE Journal of Structural Engineering* 129, 5, 2003, pp 615-625.

[6] CNR. “CNR-DT 200/2004 – Guide for Design and Construction of Externally Bonded FRP Systems for Strengthening Existing Structures”, Consiglio Nazionale delle Ricerche, Rome, Italy, 2004, 154 pp.